High-Frequency Modeling and Optimization of E/O Response and Reflection Characteristics of 40 Gb/s EML Module for Optical Transmitters

Chengzhi Xu, Y.Z. Xu,Yanli Zhao, Kunzhong Lu, Weihua Liu, Shibing Fan, Hui Zou, and Wen Liu

A complete high-frequency small-signal circuit model of a 40 Gb/s butterfly electroabsorption modulator integrated laser module is presented for the first time to analyze and optimize its electro-optic (E/O) response and reflection characteristics. An agreement between measured and simulated results demonstrates the accuracy and validity of the procedures. By optimizing the bonding wire length and the impedance of the coplanar waveguide transmission lines, the E/O response increases approximately 5% to 15% from 20 GHz to 33 GHz, while the signal injection efficiency increases from approximately 15% to 25% over 18 GHz to 35 GHz.

Keywords: Electroabsorption modulator integrated laser (EML), E/O response, reflection characteristics, circuit model, butterfly packaging, optical transmitter.

Manuscript received Aug. 15, 2011; revised Dec. 23, 20111; accepted Jan. 9, 2012.

This work was supported in part by the National High Technology Research and Development Program of China (Grant No. 2008AA01Z207), the Natural Science Foundation of Hubei Province, China (Grant No. 2010CDB01606), the Research Funds for the Central Universities (HUST: No. 2011QN036), National High Technology Developing Program of China under Grant (No. 2009AA03Z418) and National Natural Science Foundation of China (No.: 60607006).

Chengzhi Xu (phone: +86 15871693005, xuchengzhixu@163.com), Yanli Zhao (yanlizhao@mail.hust.edu.cn), Weihua Liu (whliu@wtd.com.cn), and Wen Liu (wen.liu@accelink.com) are with Wuhan National Laboratory for Optoelectronics, College of Optoelectronic Science and Engineering, Huazhong University of Science and Technology, Wuhan, China .

Y.Z. Xu (yzxu@wtd.com.cn), Kunzhong Lu (klu@wtd.com.cn), Shibing Fan (sbfan@wtd.com.cn), and Hui Zou (zouhui@wtd.com.cn) are with Wuhan Telecommunication Devices Co. Ltd., Wuhan, China.

http://dx.doi.org/10.4218/etrij.12.0111.0516

I. Introduction

The single channel data rate of the optical communication system has increased from 10 Gb/s to 40 Gb/s and can reach up to 100 Gb/s. Achieving these faster rates requires optoelectronic components with higher performance in terms of stability, modulation bandwidth, extinction ratio, and package size. The monolithic integration of an electroabsorption modulator (EAM) and a distributed feedback laser is a promising solution due to the component's compact size, high optical output power, high modulation bandwidth, low cost, low driving voltage operation, and excellent extinction ratio [1]-[4]. For a 40 Gb/s application, the bandwidth margin of the electroabsorption modulator integrated laser (EML) chip is small; therefore, careful radio frequency design is needed to achieve the performance for the packaged module. For high-speed application, the optoelectronic components inside the package may interfere with each other if the structure of the package is not chosen properly. Two types of mainstream packaging are popular for high-speed optoelectronic devices: the butterfly package [5] and the transistor outline (TO) package [6], [7]. The high-frequency electric signal of the TO-type package is fed in through the RF pin, and its microwave performance can hardly meet the requirements of 40 Gb/s applications. Nevertheless, the size of the TO-type package is too small to dissipate the heat generated by a high-power thermoelectric cooler. To meet the high-frequency electro-optic (E/O) response requirement, the radio frequency electric signal input ports of a 14-pin butterfly package housing have been replaced by high-

frequency coaxial connectors, such as V or GPPO connectors, which have better microwave performance. This packaging technique is also widely deployed in high-speed transponders, transmitters, small form modules, and some novel optoelectronics components.

To understand the characteristics and behaviors under various configurations inside a module, it is very important to construct a high-frequency model of the modules. Regarding earlier models, the presenting researchers derived significant analysis of the frequency characteristics of the laser module. Lee and others proposed a complete small-signal model of a butterfly-type 2.5 Gb/s DFB laser module [8]. Delpiano and others described a high-frequency model of a DFB laser module with which they analyzed and optimized the main factors contributing to the bandwidth limitation of the module [9]. A small-signal equivalent TO-type package laser module was presented by Zhu and others, where the effects of each element on the high-frequency response were analyzed [10]. Great improvement and low cost packaging can be achieved with these proposed models. However, there is so far no report or analysis on a model of an EML butterfly package with a high-frequency coaxial connector.

In this paper, we propose a complete high-frequency small-signal circuit model of a 40 Gb/s EML butterfly package with a V-type coaxial connector and analyze its frequency characteristics. The 40 Gb/s EML module includes a V connector butterfly package, a high-frequency submount, bonding wires, and an EML chip. A test platform for an EML chip on a submount and an EML module is built. E/O response (S21) and reflection characteristics (S11) are measured and compared with the simulated data to validate the circuit model. This high-frequency model is employed to optimize the bonding wire length and the impedance of the coplanar waveguide (CPW) transmission lines, and the E/O response and the reflection performance are greatly improved.

II. Model of EML Chip and Measurement Setup

1. Small-Signal Model of EML Chip

Figure 1 shows a typical structure of an InGaAlAsP multiple-quantum-well (MQW) EML chip. An InGaAlAsP MQW EML chip is grown by a combination of selective area growth and several other epitaxial growth steps by means of metal organic chemical vapor deposition. The EML consists of a DFB laser section that operates in the CW mode, and an EAM section that modulates the output light. The two sections are separated by an isolation section. The small-signal equivalent circuit model of the EML chip is derived based on this structure, as shown in Fig. 2.

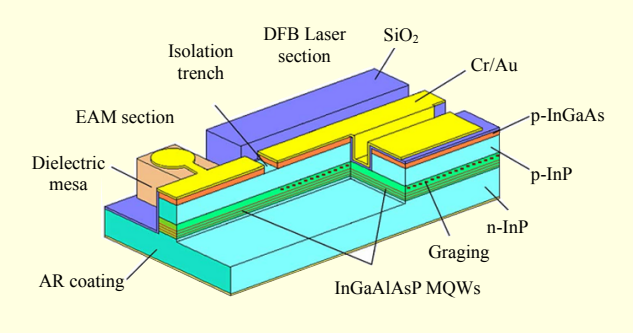

Fig. 1. Typical structure of InGaAlAsP MQW EML.

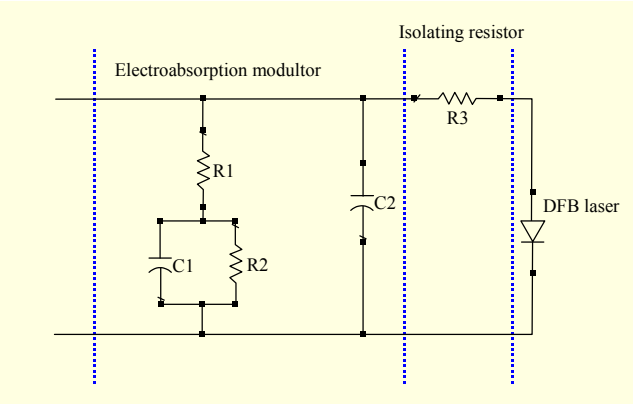

Fig. 2. Small-signal equivalent circuit model of EML chip.

Capacitance C2 in the model represents the parasitic capacitance generated by the solder joint, while C1 represents the junction capacitance, which consists of the capacitance of the MQW active region and the capacitance of the indium phosphate layers. R1 and R2 represent the device resistance and the resistance generated by photocurrent, respectively. The EAM section operation is reverse biased and connected to the DFB laser through an isolation trench, which has a large resistance (represented by R3, as in Fig. 2). The resistance of the isolation trench is usually larger than 3 kΩ; therefore, the DFB laser will not be interfered with by the high-frequency characteristic of the EAM. The DFB laser can then be represented by a PIN diode.

2. Network Theoretical Description

The measurement configuration for the EML module can be divided into three cascaded networks: 1) the network of the test fixture, the package parasitic element, and the intrinsic EAM in the EML chip (represented by network P); 2) the intrinsic network of the laser in the EML chip (represented by network L); and 3) the network of the receiver (represented by network R). The scattering parameters of the EML and the receiver can be written as [11]

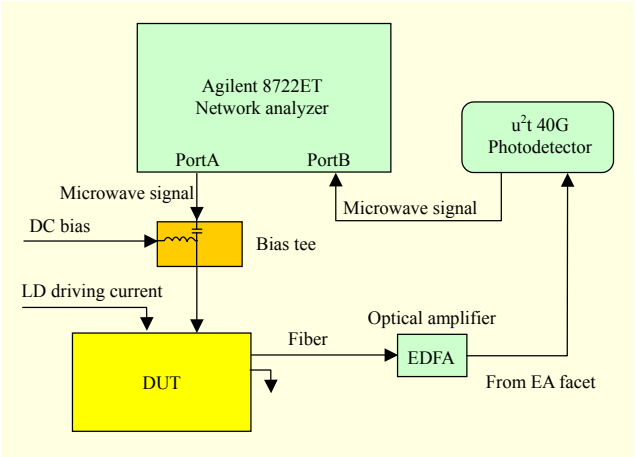

Fig. 3. Measurement setup for DUT.

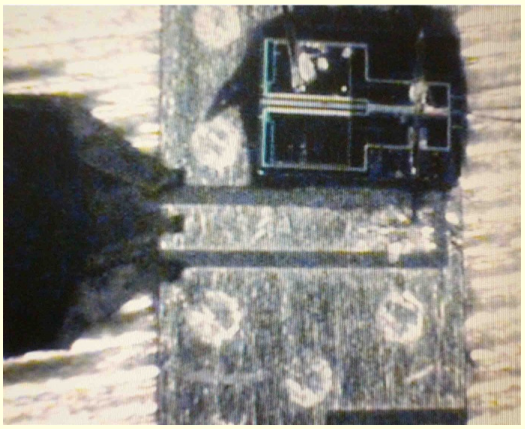

Fig. 4. Image of test EML chip on submount.

$$S^L = \begin{bmatrix} S_{11}^L, 0 \\ S_{21}^e, 0 \end{bmatrix}, \quad S^R = \begin{bmatrix} 0, & 0 \\ S_{21}^R, S_{22}^R \end{bmatrix}. \tag{1}$$

The intrinsic laser can be negligible compared with the serial resistance R3, and S_{11}^L can be regarded as –1[12]. Meanwhile, at high reverse bias currents, the receiver can be replaced by an open circuit [13], and S_{22}^R can be regarded as 1. The T-matrix of the whole measured EML module can be written as

$$T = T^P T^{LR} = \frac{1}{S_{21}^P S_{21}^R} \begin{bmatrix} S_{12}^P S_{21}^P - S_{11}^P S_{22}^P, S_{11}^P \\ -S_{22}^P, \quad 1 \end{bmatrix} \begin{bmatrix} 0, S_{11}^L \\ 0, 1 \end{bmatrix}$$

$$= \frac{1}{S_{21}^P S_{21}^R} \begin{bmatrix} 0, S_{11}^P - S_{12}^P S_{21}^P + S_{11}^P S_{22}^P \\ 0, 1 - S_{22}^P \end{bmatrix}. \tag{2}$$

By transforming the above T-matrix to S-parameters, we have

$$S_{11} = \frac{S_{11}^P - S_{12}^P S_{21}^P + S_{11}^P S_{22}^P}{1 + S_{22}^P}, \quad S_{21} = \frac{S_{21}^P S_{21}^R}{1 + S_{22}^P}. \tag{3}$$

From (3), we can see that the reflection coefficient depends only on the cascade of the test fixture, the package parasitic element, and the intrinsic EAM in the EML chip. Therefore, we can extract the values of these fixtures, the package parasitic element, and the intrinsic parameters of the EAM from the measured S11 by a traditional curve fitting method [14].

3. Measurement Setup

The measurement setup is shown in Fig. 3. The high-frequency microwave signal with a frequency of up to 40 GHz is fed through a V-type connector to a butterfly-packaged EML module or through a high-frequency CPW probe (GGB 58801) to the submount with the EML chip. The microwave signal is generated by a network analyzer (Agilent 8722ET). A reverse voltage is loaded to the EAM by a DC bias tee. The output light is amplified by an EDFA and then converted to an electrical RF signal by a photodetector (u^2t 40G), which is connected to a network analyzer. In theory, we can test the total frequency response of the test fixture, the receiver, and the device under test (DUT). A de-embedding method is employed in this test. The responses of the test fixture and the receiver are pre-embedded in the test system so that we can directly obtain the small-signal response of the DUT. The S21 result is simply the E/O response of the DUT in the test. The image of the test EML chip on the submount is shown in Fig. 4.

III. Small-Signal Model of 40 Gb/s Butterfly EML Module

1. EML Chip on Submount

Figure 5 shows the small-signal circuit model of the EML chip on the submount. Inductor L1 and resistor R4 represent the inductance and resistance of the bonding wire, which connects the EAM electrode of the chip to the signal line of the CPW on the submount. C3 represents the capacitance of the submount. There is a 50 Ω thin film resistor represented by R5, shunted with the EML chip on the submount to ensure the total impedance of around 50 Ω. The inductance and resistance of the bonding wire between the EA electrode of the chip and the 50 Ω thin film resistor are represented by L2 and R6, respectively. With the laser diode biased at 60 mA and the EAM reverse biased at –2.1 V, the S11 and S21 of the EML chip on the submount are measured, as shown in Fig. 6. The commercial high-frequency computer-aided design package (Advanced Design System) is used to extract the parameters by a traditional curve fitting method. The extracted values of the small-signal model for the EML chip on the submount are shown in Table 1. The measured curves agree well with the

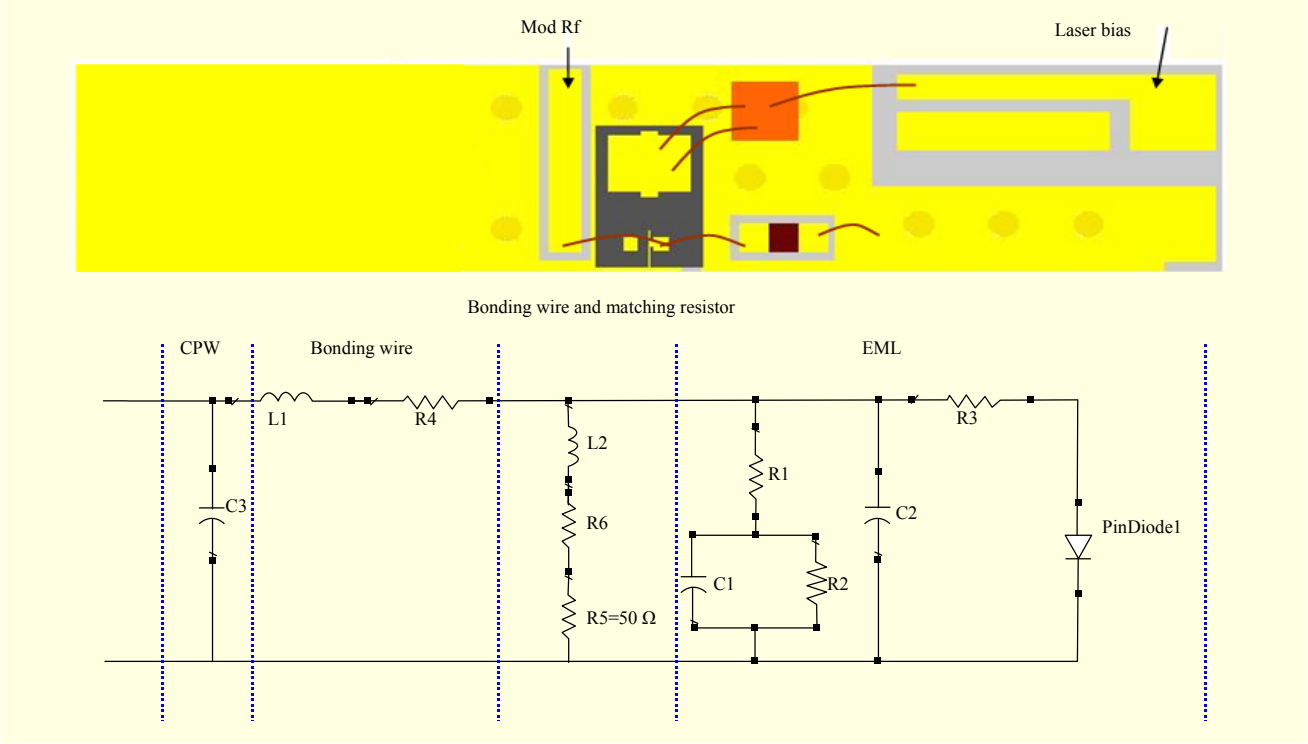

Fig. 5. Schematic and small-signal model of EML chip on submount.

Table 1. Extracted values of small-signal model for EML chip on submount.

Components	Extracted values	Components	Extracted values
L1 (nH)	0.256	R1 (Ω)	13.68
L2 (nH)	0.161	R2 (Ω)	132.23
C1 (pF)	0.021	R3 (Ω)	3200.00
C2 (pF)	0.054	R4 (Ω)	1.74
C3 (pF)	0.102	R5 (Ω)	50
R6 (Ω)	0.667		

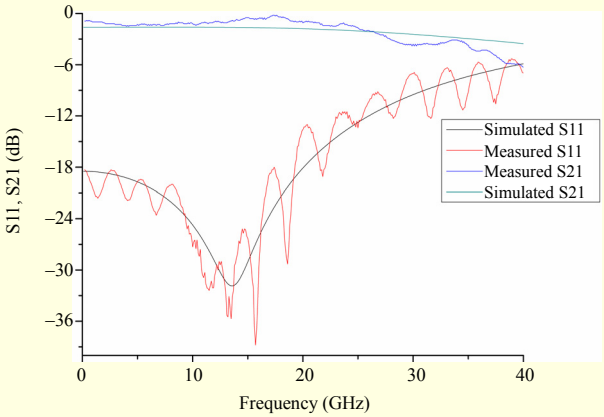

Fig. 6. Simulated and measured S11 and S21 at a current of 60 mA, reverse bias at –2.1 V.

fitting curves.

2. Small-Signal Circuit Model of Complete Butterfly 40 Gb/s EML Modules

The RF part of the EML module consists of an EML chip, a submount with a CPW, and a submount with a microstrip line that connects high-frequency signals from a V-type high-frequency coaxial connector with a CPW on the submount. The optical output beam from the EML chip is coupled with a single-mode fiber that has an optics system containing two aspherical lenses. A CPW is used to optimize the impedance characteristic of the device and improve the frequency response of the module. For a complete small-signal circuit model of the butterfly 40 Gb/s EML module, we combine the small-signal model of the EML chip on the submount with parasitic components, which include a high-frequency V coaxial connector, a microstrip line, a CPW, and bonding wires. Figure 7 shows the complete small-signal circuit model of the EML module. Based on the network theory as described in [11], we have the element values listed in Table 2. Figure 8 shows the measured and simulated data, which demonstrates

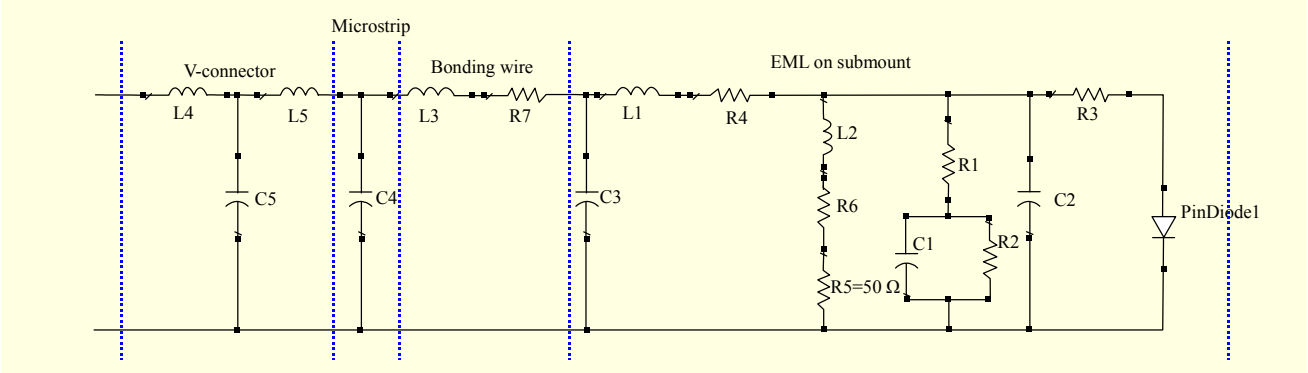

Fig. 7. Schematic drawing and small-signal model of complete butterfly-type 40 Gb/s EML modules.

Table 2. Extracted parameters of the complete small-signal model for EML module.

Parameter	Description	Value
L3 (nH)	Inductance from bonding wire that connects microstrip to CPW	0.05
L4, L5 (nH)	Inductance from high-frequency V-type connector	0.002
R7 (Ω)	Resistance from bonding wire that connects microstrip to CPW	0.30
C4 (pF)	Capacitance from microstrip	0.002
C5 (pF)	Capacitance from high-frequency V-type connector	0.020

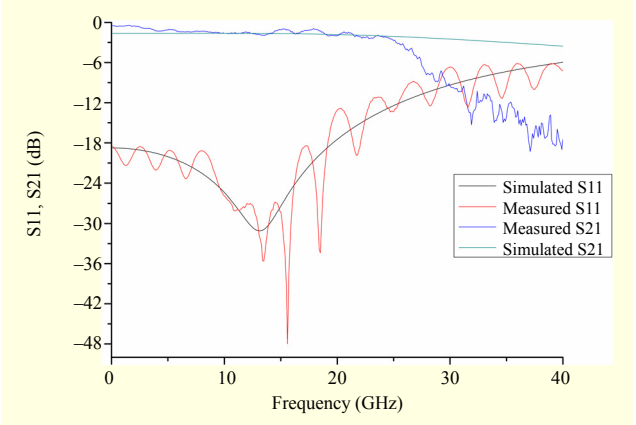

Fig. 8. Simulated and measured S11 and S21 of butterfly 40 Gbps EML module with 60 mA current, and –2.1 V reverse bias.

agreement at the measuring frequency range up to 28 GHz.

IV. Effects of Bonding Wires and Optimizing of Module

1. Effects of Bonding Wire on Module Based on Model

As we know, the bonding wire will introduce parasitic inductance and this cannot be neglected, especially in the package with a frequency over 10 GHz. The distance between the EML chip and the 50 Ω thin film resistor is relatively short, and so is the distance between the CPW and the microstrip. Therefore these bonding wires can be taken as fixed values. L1, which connects the EA electrode of chip to the CPW on the submount, becomes the only key parasitic inductance. In our package, the inductance of a typical single diameter of 1 mil wire is about 0.7 nH/mm. The lengths of L2 and L3 are 0.23 mm and 0.07 mm, respectively. Figure 9 shows the simulated S11 of the module in terms of bonding wire length L1. The length of L1 should not exceed 0.4 mm so as to maintain a return loss below –10 dB for a frequency range up to 28 GHz.

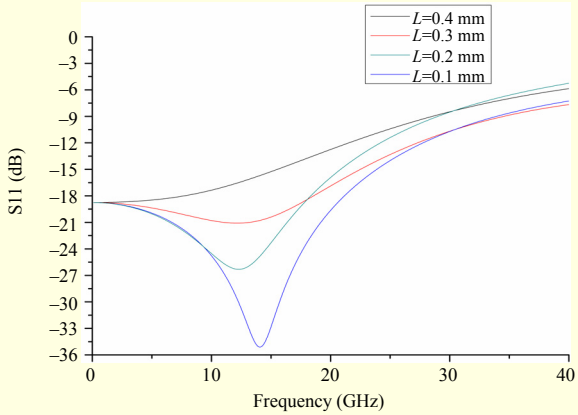

Fig. 9. Simulated S_{11} with variable wire bonding lengths of L1.

2. Optimization of the Module

Good E/O response and low input return loss depend not only on the EML chip itself but also on other package components. For a typical EML module, a characteristic impedance of the CPW transmission lines on an aluminium nitride submount is selected as 50 Ω. From this high-frequency small-signal circuit model, we found that there was a large impedance mismatch between the EML chip and such

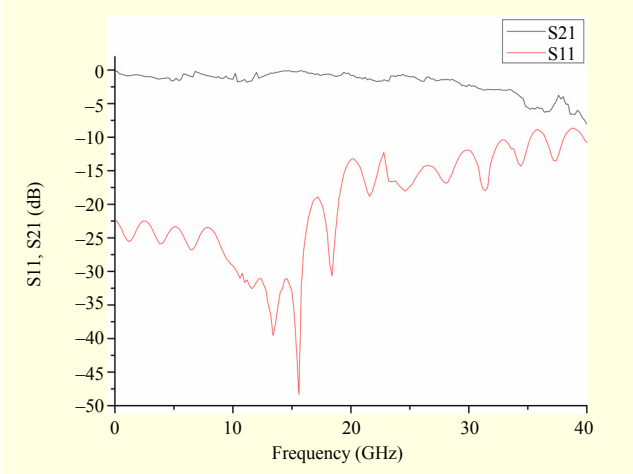

Fig. 10. Measured frequency response of EML module with optimized CPW.

conventional CPW transmission lines especially at a high frequency. The RF performance of the module can be improved by optimizing the impedance match of the EML chip and the CPW. However, the impedance of the EML chip is not easy to modify, since changing the impedance of the EML chip will add other trade-offs. For example, if we further reduce the capacitance of the EML chip to improve the RF response by reducing the EA modulator length, other characteristics such as extinction ratio will degrade. Therefore, to reduce the impedance mismatch, it is proposed here to optimize the CPW transmission lines on the submount by using the proposed model. It is found that an optimized 42 Ω characteristic impedance of the CPW transmission lines has the best match with the EML chips. Figure 10 shows the measured frequency response of the EML module with the optimized CPW. We can see that the input return loss is below –10 dB up to 35.2 GHz, and the 3 dB frequency response bandwidth is 33.1 GHz. In the latter case, the signal injection efficiency increases from approximately 15% to 25% over 18 GHz to 35 GHz, while the modulation bandwidth increases approximately 5% to 15% from 20 GHz to 33 GHz. With this model we can improve the RF performance of the EML module by optimizing the design and the matching of different components one by one in the package.

V. Conclusion

In this paper, we proposed a small-signal equivalent circuit model of a 40 Gb/s butterfly EML module. Our method employed a step-by-step measurement and fitting procedure to build the model. In each step, an agreement between measurement and simulation results was achieved, and the stability of the extracted values of each parasitic element demonstrated the accuracy of the model. The proposed model was used to optimize the length of the bonding wire and the CPW submount, while the E/O and reflection characteristics of the EML module were greatly improved.

References

[1] H.G. Yun et al., "Fabrication and Characteristics of 40 Gb/s Traveling-Wave Electroabsorption Modulator-Integrated DFB Lasers Modules," *IEEE Trans. Adv. Packag.,* vol. 31, no. 2, May 2008, pp. 351-356.

[2] Y. Akage et al., "Wide Bandwidth of over 50 GHz Traveling-Wave Electrode Electroabsorption Modulator Integrated DFB Lasers," *IEEE Electron. Lett.,* vol. 37, no. 5, 2001, pp. 299-300.

[3] H. Kawanishi et al., "EAM-Integrated DFB Laser Modules with More Than 40-GHz Bandwidth," *IEEE Photon. Tech. Lett.,* vol. 13, no. 9, Sep. 2001, pp. 954-956.

[4] H. Feng et al., "40 Gb/s Electro-Absorption-Modulator- Integrated DFB Laser with Optimized Design," *Proc. Optical Fiber Communication (OFC)*, Paper WV4, 2002, pp. 340-341.

[5] H.-G. Yun et al., "Fabrication and Characteristics of 40 Gb/s Traveling-Wave Electroabsorption Modulator-Integrated DFB Laser Modules," *Proc. 56th Electron. Components Technol Conf.,* 2006.

[6] A. Ebberg, F. Auracher, and B. Borchert, "10 Gbit/s Transmission Using Directly Modulated Uncooled MQW Ridge Waveguide DFB Lasers in TO Package," *IEEE Electron. Lett.,* vol. 36, no. 17, 2000, pp. 1476-1477.

[7] S.H. Hall et al., "VCSEL Electrical Packaging Analysis and Design Guidelines for Multi-GHz Applications," *IEEE Trans. Compon. Packag. Technol. B,* vol. 20, no. 3, Aug. 1997, pp. 191-201.

[8] J. Lee et al., "A Complete Small-Signal Equivalent Circuit Model of Cooled Butterfly-Type 2.5 Gbps DFB Laser Modules and Its Application to Improve High Frequency Characteristics," *IEEE Trans. Adv. Packag.,* vol. 25, no. 4, Nov. 2002, pp. 543-548.

[9] F. Delpiano et al., "High Frequency Modeling and Characterization of High Performance DFB Laser Modules," *IEEE Trans. Comp., Packag., Manufact., Technol. B,* vol. 17, no. 3, Aug. 1994, pp. 412-417.

[10] C. Chen et al., "Characterization of Parasitics in TO-Packaged High-Speed Laser Modules," *IEEE Trans. Adv. Packag.*, vol. 30, no. 1, 2007, pp. 97-103.

[11] P.D. Hale and D.F. Williams, "Calibrated Measurement of Optoelectronic Frequency Response," *IEEE Trans. Microw. Theory Tech.,* vol. 51, no. 4, Apr. 2003, pp. 1422-1429.

[12] R.S. Tucker, "High-Speed Modulation of Semiconductor Lasers," *J. Lightwave. Technol.,* vol. LT-3, no. 6, Dec. 1985, pp. 1180-1192.

[13] G. Wang et al., "Analysis of High Speed PIN Photodiodes S-Parameters by a Novel Small-Signal Equivalent Circuit Model,"

IEEE Microw. Compon. Lett., vol. 12, no. 10, Oct. 2002, pp. 378-380.

[14] P.A. Morton et al., "Frequency Response Subtraction for Simple Measurement of Intrinsic Laser Dynamic Properties," *IEEE Photon. Technol. Lett.,* vol. 4, no. 2, Feb. 1992, pp. 133-136.

Chengzhi Xu received his BS in physics from Huaibei Normal University, Huaibei, China, in 2007. He is currently pursuing a PhD in optoelectronic information engineering at the Wuhan National Laboratory for Optoelectronics, College of Optoelectronic Science and Engineering, Huazhong University of Science and Technology, Wuhan, China. From 2008 to 2012, he was with the State Key Laboratory of Optical Communication Technologies and Networks, Wuhan Telecommunication Devices Co. Ltd., and participated in a research program regarding the packaging of a 40 Gb/s and 100 Gb/s EML module integrated driver IC. His current research interests include microwave measurement, modeling, thermal behavior, and packaging design of high-speed optoelectronic devices and modules.

Y.Z. Xu is a professor in the Wuhan National Laboratory for Optoelectronics, College of Optoelectronic Science and Engineering, Huazhong University of Science and Technology, Wuhan, China. He received his BS in engineering from Huazhong University of Science and Technology in 1990 and PhD in electrical engineering from The Hong Kong Polytechnic University, Kowloon, Hong Kong, SAR China, in 1999, respectively. In Nov. 1999, he joined the Wuhan Research Institute of Posts & Telecommunications and led a team pioneering in advanced micro-optics components in China. Dr. Xu worked for Lightwaves 2020, Milpitas, California, USA, on advanced devices based on fiber Bragg grating from Aug. 2000 to April 2001. He is a member of the IEEE, the Optics Society of America, the Chinese Society of Communication, and the Chinese Society of Optics.

Yanli Zhao received his PhD in physics from Zhejiang University, China, in 2002. From 2002 to 2005, he was with Wuhan Telecommunication Device Copany (WTD), where he worked as an engineer on optical communication devices. In 2005, he joined the Venture Business Laboratory (VBL), Nagoya University, Japan, where he worked on nano-material fabrication and its application. In 2007, he joined Wuhan National Laboratory for Optoelectronics (WNLO), Huazhong University of Science and Technology. At present, he is a research professor actively involved in nanomaterial and photodevices.

Kunzhong Lu received his BS and MS in physics from Wuhan University,Wuhan, China, in 2004 and 2007, respectively. He received his PhD in physics from the University of Connecticut, Storrs, Mansfield, CT, USA, in 2001. He worked for Multiplex Inc. in NJ, USA from 2001 to 2010, and he is currently the Chief Scientist in chips and components technologies in the State Key Laboratory of Optical Communication Technologies and Networks in the Wuhan Research Institute of Posts & Telecommunications, Wuhan, China. His expertise is in optoelectronics chips and device design, simulation, and testing. His research interests include theoretical analysis and simulation of high-speed and high-power semiconductor lasers, optoelectronics device packaging design, and photonic integrated chips and devices.

Weihua Liu received his MS from Shaanxi Normal University, Xi'an, Shaanxi, China, in 2006. From 2006 to 2009, he was an instructor at Wuhan Polytechnic University. He is currently working toward a PhD at the Wuhan National Laboratory for Optoelectronics, Huazhong University of Science and Technology. He also is an R&D engineer at Wuhan Telecommunication Device Co. Ltd.. His current research interests include 40/100G optoelectronics devices packaging and integrated optical elements and systems.

Shibing Fan received his BS in physics from Wuhan University in Wuhan, China, in 1997. Since 2005, he has been a senior researcher with Wuhan Research Institute of Posts & Telecommunications, Wuhan, China. His current research interests include high-speed optical modules and systems.

Hui Zou received his BS in physics from Three Gorges University, Yicang, China, in 2000. In 2008, he received his MS in communication and information systems from Wuhan Research Institute of Posts &Telecommunications, Wuhan, China. His current research interests include high-speed optical modules and systems.

Wen Liu is a professor in the Wuhan National Laboratory for Optoelectronics, College of Optoelectronic Science and Engineering, Huazhong University of Science and Technology, Wuhan, China. He received his BS and PhD in physics from the University of Science and Technology of China. His current research interests include optoelectronics devices, packaging, and integrated optical elements and systems.